

# Weighing the Axion with Muon Haloscopy

N. Bray-Ali\*

February 14, 2023

## Abstract

Recent measurements of muon spin precession confirm a long-standing tension with the Standard Model of particle physics. We argue that axions from the local dark matter halo of the galaxy are responsible for the tension. The argument yields a percent level prediction for the mass of the axion provided that axions are the dark matter that dominates gravitation in galaxies, galaxy clusters, and the large-scale “cosmic web” structure of the Universe.

*Essay written for Gravity Research Foundation 2023 Awards for Essays on Gravitation*

---

\*Corresponding Author. Email Address: nbrayali@msmu.edu. Mailing address: Department of Physical Sciences, Mount Saint Mary’s University, 12001 Chalon Road, Los Angeles, California 90049

# 1 Introduction

The spin of the muon precesses in a magnetic field  $B$  at frequency  $\omega_a = a_\mu(e/m_\mu)B$ , where,  $a_\mu \approx \alpha/(2\pi) \approx 1.16 \times 10^{-3}$ , and  $e/m_\mu = 2\pi \times 135$  MHz/T is the charge to mass ratio of the muon [1-4]. Compared with the electron, the muon is  $(m_\mu/m_e)^2 \approx 43,000$  times more sensitive to the hadronic leading order contribution  $a_\mu^{\text{HLO}}$  to spin precession [5, 6]. In this Essay, we show that axions in the local dark matter halo of the galaxy shift  $a_\mu$  and  $a_\mu^{\text{HLO}}$  from their standard model values. Further, we argue that the size of these axion-induced shifts explains the tension between measurements of the muon spin precession frequency [2, 3] and calculations of the frequency based on measurements of the hadronic leading order contribution [5]. Finally, we give a physical picture for the nature of axions that leads to a prediction for the mass of the axion with percent level precision and we sketch table-top experiments for testing this prediction. Our conclusion is that dark matter is made of axions.

## 2 Axion Mass

We start by expressing the axion  $A_M$  in terms of quarks and leptons  $M_H^P$  with helicity  $H = L, R$  and charge-parity check  $P = +, -$  [8]:

$$A_M = M_L^- \overline{M}_R^- - M_R^- \overline{M}_L^- - M_L^+ \overline{M}_R^+ + M_R^+ \overline{M}_L^+ \quad (1)$$

Here,  $M$  runs over the twelve known “flavors” of quarks and leptons while the charge-parity check  $P$  is  $+$  for quarks and leptons that do not feel the weak nuclear force and  $-$  for those that do. In the standard model, we find  $M_L^-$  and  $M_R^+$ , but neither  $M_L^+$  nor  $M_R^-$ , where,  $L$  is for left-handed and  $R$  is for right-handed helicity [9].

Next, we suppose that axions  $A_M$  of each kind and photons  $\gamma_H$  of each helicity formed in equal numbers in the early universe prior to baryogenesis. This fixes the ratio  $n_A/n_\gamma =$

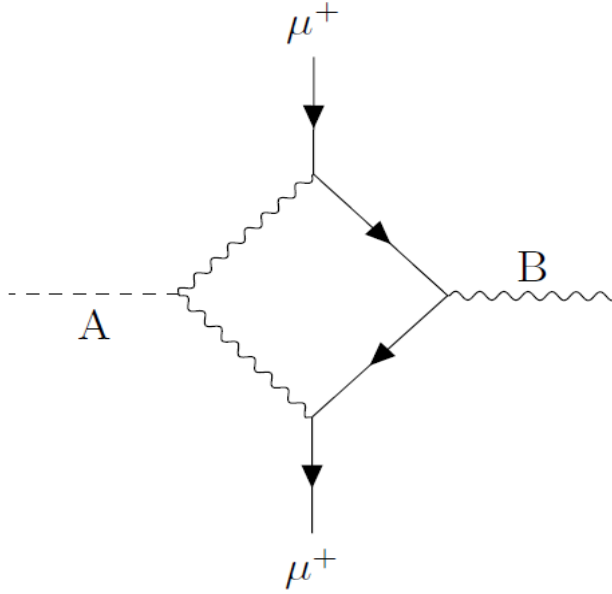


Figure 1: Halo axion  $A$  collides with virtual photon or vector meson dressing vertex of positive muon  $\mu^+$  and magnetic field  $B$ .

$|M|/|H| = 6$  of axions to photons and gives the axion mass  $m_A$  ( $\hbar = c = 1$ ) [10]:

$$m_A = 2.70 kT_\gamma \left( \frac{n_A}{n_\gamma} \right)^{-1} \frac{\Omega_A h^2}{\Omega_\gamma h^2} = (0.508 \pm 0.004) \text{ eV}, \quad (2)$$

where,  $T_\gamma = (2.7255 \pm 0.0006) \text{ K}$  is the present photon temperature[11],  $\Omega_\gamma h^2 = 2.473 \times 10^{-5}$  is the photon energy density parameter and  $\Omega_A h^2 = 0.11882 \pm 0.00086$  is that of the axions assuming they saturate the dark matter [12].

### 3 Muon Haloscopy

Figure 1 shows how axions in the local halo shift muon spin precession [2, 3, 4]. Acting as a background field  $\tilde{\phi}_A(q_A)$  with on-shell four-momentum  $q_A^2 = m_A^2 \ll m_\mu^2$ , the axion  $A$  couples to the virtual photon dressing the vertex of the positive muon  $\mu^+$  and the magnetic field  $B$ . The shift of the spin precession frequency  $\Delta a_\mu$  grows with the axion-photon coupling

$g_{A\gamma\gamma}$  [13]:

$$\frac{\Delta a_\mu}{a_\mu} = m_A^2 g_{A\gamma\gamma} \tilde{\phi}_A(q_A) = \pm m_A g_{A\gamma\gamma} \sqrt{\rho_A N_\mu V_\mu T_\mu} \quad (3)$$

where, the axion field strength  $|\tilde{\phi}_A(q_A)|^2 \approx \phi_A^2 N_\mu V_\mu T_\mu$  is fixed by the axion energy density  $\rho_A = \phi_A^2 m_A^2$ , the volume  $V_\mu$  of the muon beam, the lifetime  $T_\mu$  of the muon in the axion rest-frame, and the average number of muons  $N_\mu$  during spin precession. The sign of the shift  $\Delta a_\mu$  in Eq. (3) switches along with the axion field  $\tilde{\phi}_A(q_A)$  under the symmetries  $P$ ,  $T$ ,  $CP$ , and  $CT$  [14]. The size of the shift scales with the effective four-volume  $NVT$  of the muon beam.

The shift in the muon spin precession frequency  $\Delta a_\mu$  due to axions in the local dark matter halo of the galaxy has roughly the right size to resolve the tension  $a_\mu(\text{Exp}) - a_\mu(\text{SM}) = (251 \pm 59) \times 10^{-11}$  between experiments (Exp) [2, 3] and standard model calculations (SM) [5, 6]. Assuming axions saturate the local halo, their energy density  $\rho_A = (0.30 \pm 0.03) \text{ GeV/cm}^3$  follows from galactic orbital dynamics and other astrophysical constraints [15]. The axion-photon coupling strength is  $g_{A\gamma\gamma} = (0.68 \pm 0.02) \times 10^{-10} \text{ GeV}^{-1}$  for the axion mass  $m_A = (0.508 \pm 0.004) \text{ eV}$  [16]. Combining these inputs, we find that the shift  $\Delta a_\mu = (170 \pm 10) \times 10^{-11}$  of the muon spin precession frequency due to axions in the local dark matter halo of the galaxy roughly resolves the tension between experiment and the standard model [19].

Figure 1 also shows how axions from the local dark matter halo of the galaxy shift measurements of the leading order hadronic contribution  $a_\mu^{\text{HLO}}$  to muon spin precession [4, 5]. The axions collide with the  $\rho$  vector meson that dominates the hadronic production from electron-positron annihilation whose cross-section enters the standard model calculation of  $a_\mu^{\text{HLO}}$ . The collisions convert the short-lived  $\rho$  meson, which produces mainly charged pion  $\pi^+\pi^-$  pairs, into the longer lived and slightly heavier  $\omega$  meson, which prefers to produce a neutral pion  $\pi^0$  in addition to the charged pion pair. The conversions reduce the  $\pi^+\pi^-$  hadronic production cross-section at the  $\rho$  resonance and shift the calculated value of the

leading order hadronic contribution [22]:

$$\begin{aligned}\Delta a_\mu^{\text{HLO}} &= a_\mu m_A^2 g_{A\rho\omega} \tilde{\phi}_A(q_A) \\ &= \frac{\alpha}{3} \Delta a_\mu \sqrt{\frac{m_\rho}{\Gamma_\rho^{ee}} \frac{m_\omega}{\Gamma_\omega^{ee}} \frac{N_e}{N_\mu} \frac{V_e}{V_\mu} \frac{T_e}{T_\mu}},\end{aligned}\tag{4}$$

where, the mass of vector meson  $V = \rho, \omega$  is  $m_V$ , the partial width  $\Gamma_V^{ee}$  gives the rate that  $V$  produces an electron-positron pair,  $N_e$  is the number of electrons and positrons in each colliding bunch,  $V_e$  is the luminous volume they create, and  $T_e$  is the time it takes the bunches to cross during the collision [21,22]. The shift  $\Delta a_\mu^{\text{HLO}}$  in the hadronic contribution combines with the shift  $\Delta a_\mu$  in the spin precession frequency to give a gap between experiment and the standard model  $\Delta a_\mu + \Delta a_\mu^{\text{HLO}} = (283 \pm 17) \times 10^{-11}$  that is quite close to the observed tension [25].

## 4 Infrared Haloscopy

Figure 2 shows how the axion converts infrared photons into radio-frequency magnetic fields. From Eq. (2) we find that the wavelength  $\lambda_A = 2\pi/m_A = (2441 \pm 19)$  nm corresponding to the mass of the axion falls in the mid-infrared. Detuning the infrared light from  $\lambda_A$  by the ground-state hyperfine transition frequency of an alkali atom, such as cesium-133, we can create radio-frequency magnetic field  $B_{\text{GHz}}$  within a resonant microwave cavity surrounding a gas vapor cell [27]:

$$B_{\text{GHz}} = m_A^2 g_{A\gamma\gamma} E_{\text{IR}} \tilde{\phi}_A(q_A) = \frac{\Delta a_\mu}{a_\mu} E_{\text{IR}} \sqrt{\frac{N}{N_\mu} \frac{V}{V_\mu} \frac{T}{T_\mu}}.\tag{5}$$

Here,  $E_{\text{IR}}$  is the infrared electric field,  $N$  is the number of gas atoms,  $V$  is the volume of the microwave cavity, and  $T$  is the cavity life-time. By scanning the infrared wavelength and looking for resonant absorption of the radio-frequency magnetic field by the atoms, it is possible to measure  $\lambda_A$  and hence determine the mass of the axion directly in a table-top

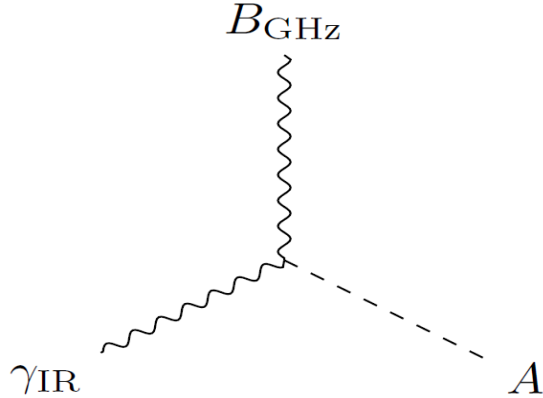


Figure 2: Halo axion  $A$  converts infrared photon  $\gamma_{\text{IR}}$  into microwave magnetic field  $B_{\text{GHz}}$

experiment to better than a percent.

Figure 3 shows how the axion allows infrared light to excite electromagnons in ferroelectric antiferromagnets such as  $\text{BiFeO}_3$ . At room temperature the strongest electromagnon resonance in  $\text{BiFeO}_3$  lies in the terahertz regime at frequency  $\omega_\theta = 2\pi \times 0.54$  THz. With increasing temperature, the electromagnon softens along with the spin density wave amplitude[28]. Looking in the infrared, we expect to see the electromagnon resonance as an absorption line in transmission through a thin sample, for example, provided the light is detuned by  $\omega_\theta$  from the axion frequency  $\omega_A = m_A = 2\pi \times (122.9 \pm 1.0)$  THz[29]. Measuring the infrared frequency that resonantly excites the electromagnon provides a table-top determination of the mass of the axion to better than a percent.

## 5 Conclusion

We conclude that the tension between measurements of muon spin precession and standard model calculations is due to axions in the local dark matter halo of the galaxy. Comparing the axion shift with the muon tension, we infer that axions saturate the local halo energy density. Symmetry and cosmology combine to give the axion mass  $m_A = (0.508 \pm 0.004)$  eV provided that dark matter is made of axions. Table-top experiments using readily available materials

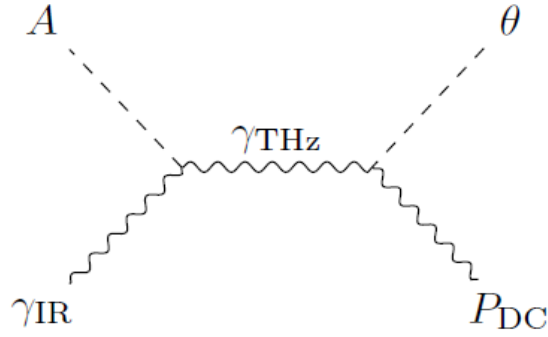


Figure 3: Halo axion  $A$  converts infrared photon  $\gamma_{\text{IR}}$  into terahertz photon  $\gamma_{\text{THz}}$  resonant with electromagnon  $\theta$  in ferroelectric antiferromagnet with polarization  $P_{\text{DC}}$ .

and devices can test this prediction and determine the mass of the axion to better than a percent. Such direct measurements would confirm that axions indeed form the dark matter that dominates the gravitation of galaxies, galaxy clusters, and the large-scale “cosmic web” structure of the Universe.

## Acknowledgements

This research was supported in part by the National Science Foundation under Grant No. NSF PHY-1748958, by the Department of Energy under grant No. DE-FG02-00ER41132, and by the Mainz Institute of Theoretical Physics within the Cluster of Excellence PRISMA+ (Project ID 39083149).

## References

- [1] J. Schwinger, On Quantum-Electrodynamics and the Magnetic Moment of the Electron, *Phys. Rev.* **73**, 416 (1948).
- [2] B. Abi, T. Albahri, S. Al-Kilani, D. Allspach, L. P. Alonzi *et al.* (Muon  $g - 2$  Collaboration), Measurement of the Positive Muon Anomalous Magnetic Moment to 0.46 ppm,

- Phys. Rev. Lett.**126**, 141801 (2021).
- [3] G.W. Bennett, B. Bousquet, H. N. Brown, G. Bunce, R. M. Carey *et al.* (Muon  $g-2$  Collaboration), Final report of the muon E821 anomalous magnetic moment measurement at BNL, Phys. Rev. D **73**, 072003 (2006).
- [4] F. Jegerlehner, *The Anomalous Magnetic Moment of the Muon*, 2nd ed. (Springer-Verlag, 2017).
- [5] T. Aoyama, N. Asmussen, M. Benayoun, J. Bijnens, T. Blum *et al.*, The anomalous magnetic moment of the muon in the standard model, Phys. Rep. **887**, 1 (2020).
- [6] Sz. Borsanyi, Z. Fodor, J. N. Guenther, C. Hoelbling, S. D. Katz *et al.*, Leading hadronic contribution to the muon magnetic moment from lattice QCD, Nature **593**,51 (2021).
- [7] R. D.Peccei, in *CP Violation*, ed. C.Jarlskog (World Scientific, 1989), pgs. 525–532.
- [8] The axions  $A_M$  are constructed to transform under  $C$ ,  $P$ , and  $T$  as  $CA_M = A_M$ ,  $PA_M = -A_M$ , and  $TA_M = -A_M$ . To check that they do so, recall that quarks and leptons  $M_H^P$  transforms as  $CM_H^P = \overline{M}_H^{\overline{P}}$ ,  $PM_H^P = M_H^{\overline{P}}$ , and  $TM_H^P = \overline{M}_H^{\overline{P}}$ .
- [9] For anti-matter, the meaning of the parity check is reversed compared to matter:  $P = +$  indicates anti-quarks and anti-leptons which *do* feel the weak force, while  $P = -$  means the anti-matter *does not* feel it. Nevertheless, the standard model correlation between helicity  $H = L, R$  and parity check  $P = +, -$  applies in the same way to anti-matter as it does to matter:  $\overline{M}_L^-$  and  $\overline{M}_R^+$  occur in the standard model while neither  $\overline{M}_L^+$  nor  $\overline{M}_R^-$  do. See, for example, M. E. Peskin and D. V. Schroeder, *An Introduction to Quantum Field Theory* (Perseus, 1995) pgs. 704–705.
- [10] P. J. E. Peebles, *Principles of Physical Cosmology* (Princeton University Press, 1993), pgs. 137–138, 158–160.

- [11] D. J. Fixsen, The Temperature of the Cosmic Microwave Background, *Astrophys. J.* **707**, 916 (2009).
- [12] N. Aghanim, Y. Akrami, M. Ashdown, J. Aumont, C. Baccigalupi *et al.* (Planck Collaboration), *Planck* 2018 Results VI. Cosmological Parameters, *A&A* **641**, A6 (2018). We use parameters from the baseline model fit to the most complete combination of available data. The results are given in *Planck* 2018 Results: Cosmological Parameter Tables, pg. 49 (May 14, 2019).
- [13] The axion  $\phi_A$  couples to photons via the term  $\mathcal{L}_{A\gamma} = \int d^3x dt g_{A\gamma\gamma} \phi_A \mathbf{E} \cdot \mathbf{B}$  in the action, where,  $\mathbf{E}$  is the electric field and  $\mathbf{B}$  is the magnetic field. We follow here the conventions of the axion theory review by R. D. Peccei [7] in which the “free” terms in the axion action take the form  $\mathcal{L}_A = \int d^3x dt [(1/2)(\partial_t \phi_A)^2 - (1/2)(\nabla \phi_A)^2 - (1/2)m_A^2 \phi_A^2]$ .
- [14] Under  $C$ ,  $PT$  and  $CPT$ , the shift  $\Delta a_\mu$ , like the axion amplitude, does not change sign.
- [15] A.-C. Eilers, D. W. Hogg, H.-W. Rix, and M. K. Ness, The Circular Velocity Curve of the Milky Way from 5 to 25 kpc, *Astrophys. J.*, **871**, 120 (2019).
- [16] The axion-photon coupling  $g_{A\gamma\gamma} f_A = C_{A\gamma} \alpha / (2\pi)$  [7] is given by the fine-structure constant  $\alpha \approx 1/137$ , the axion decay constant  $m_A f_A = (5.69 \pm 0.05) \times 10^{-3} \text{ GeV}^2$  [17] and the dimensionless constant  $C_{A\gamma} = 8/3 - (8m_d + 2m_u) / (3m_d + 3m_u) = 0.66 \pm 0.02$ , where, the light quarks have mass ratio  $m_u/m_d = 0.485 \pm 0.019$  [18].
- [17] M. Gorghetto and M. Villadoro, Topological susceptibility and QCD axion mass: QED and NNLO corrections. *J. High Energ. Phys.* **2019**, 33 (2019).
- [18] Z. Fodor, C. Hoelbig, S. Krieg *et al.*, Up and Down Quark Masses and Corrections to Dashen’s Theorem from Lattice QCD and Quenched QED, *Phys. Rev. Lett.* **117**, 082001 (2016).

[19] For the muon beam at Fermilab E989 (FNAL) [2], the volume is  $V = 2\pi^2 R\sigma_x\sigma_y = 3.12 \times 10^4 \text{ cm}^3$ , where,  $R = 711 \text{ cm}$  is the radius of the central orbit of muons in the ring,  $\sigma_x = 1.78 \text{ cm}$  is the radial width of the beam, and  $\sigma_y = 1.25 \text{ cm}$  is the vertical width[2, 20, 21]. The average number of muons is  $N = \frac{4}{9}N_0e^{-t_{\text{fill}}/(\gamma\tau_\mu)} \approx \frac{4}{9} \times 4340 = 1930$ , where,  $N_0 \approx 6920$  is the number of muons in the ring at the start of the fill, and  $t_{\text{fill}} \approx 30 \mu\text{sec}$  is the time it takes to fill the ring[2, 20]. The muon life-time in the haloscope rest frame is  $T = \gamma_\mu\tau_\mu = 64.4 \mu\text{sec}$ , where,  $\gamma_\mu \approx p_\mu/(m_\mu c) = 29.3$  is the muon time dilation factor,  $p_\mu = 3.10 \text{ GeV}$  is the muon momentum,  $m_\mu = 0.106 \text{ GeV}$  is the muon rest mass, and  $\tau_\mu = 2.20 \mu\text{sec}$  is the muon life-time at rest[2]. For the measurements at Brookhaven E821 (BNL) [3], we estimate  $N = 1290$ ,  $\sigma_x = 2.10 \text{ cm}$ ,  $\sigma_y = 1.53 \text{ cm}$  (J. Mott, private communication). To find the shift of muon spin precession from halo axions, we first computed  $|\Delta a_\mu(\text{FNAL})| = (171 \pm 10) \times 10^{-11}$  and  $|\Delta a_\mu(\text{BNL})| = (167 \pm 10) \times 10^{-11}$  for each experiment using Eq. (3). Next we took the average of the two experiments to obtain  $\Delta a_\mu$ , since the shifts essentially agree. Finally, the uncertainty in the shift is set mainly by the axion-photon coupling and axion energy density. These uncertainties are correlated between the two experiments, so we take the uncertainty of  $\Delta a_\mu$  to match that of the shifts seen by the individual experiments.

[20] T. Albahri, A. Anastasi, K. Badgley, S. Baessler, I. Bailey *et al.* (Muon  $g - 2$  Collaboration), Beam dynamics corrections to the Run-1 measurement of the muon anomalous magnetic moment at Fermilab, *Phys. Rev. Accel. Beams* **24**, 044002 (2021).

[21] T. Albahri, A. Anastasi, A. Anisenkov, K. Badgley, S. Baessler *et al.* (Muon  $g - 2$  Collaboration), Measurement of the anomalous precession frequency of the muon in the Fermilab Muon  $g - 2$  Experiment, *Phys. Rev. D* **103**, 072002 (2021).

[22] We follow the analysis reviewed by R. D. Peccei [7] and set the ratio of axion couplings  $g_{A\rho\omega}/g_{A\gamma\gamma} = g_{\pi\rho\omega}/g_{\pi\gamma\gamma}$  to match that of the neutral pion. Vector meson dominance [23] gives the pion ratio in terms of the  $\rho$  and  $\omega$  vector meson partial widths for electron-

positron pair production, as shown in Eq. (4). The electron-positron quantities entering Eq. (4) may be expressed in terms of the collider parameters [23]:  $N_e = \sqrt{N_+N_-}$  where  $N_+(N_-)$  is the number of positrons (electrons) per bunch,  $V_e = 8\pi\sigma_x\sigma_y\sigma_z$  where  $\sigma_x, \sigma_y, \sigma_z$  are the horizontal, vertical, and longitudinal sizes of the bunch at the interaction point, and  $T_e = 2\sigma_z/c$ .

[23] R. P. Feynman, *Photon-Hadron Interactions* (Perseus, 1972), pp. 82–85 introduces the couplings  $g_V = \alpha\sqrt{4\pi m_V/(3\Gamma_V^{ee})}$  for  $V = \rho, \omega$  and pp. 96–97 expresses the pion amplitude ratio  $g_{\pi\rho\omega}/g_{\pi\gamma\gamma} = g_\rho g_\omega/(4\pi e^2)$  in terms of these couplings and the electric charge  $e$ . Note that  $e^2 = \alpha = 1/137$  in Feynman’s conventions.

[24] V. Shiltsev and F. Zimmerman, 32. High Energy Collider Parameters in P. A. Zyla *et al.* (Particle Data Group), *Prog. Theor. Exp Phys.* **2020**, 083C01 (2021).

[25] The meson parameters are as follows [26]:  $m_\rho = 775$  MeV,  $m_\omega = 783$  MeV,  $\Gamma_\rho^{ee} = \Gamma_\rho \times \text{B.R.}(\rho \rightarrow e^+e^-) = (147 \text{ MeV})(4.72 \times 10^{-5}) = 6.94$  keV, and  $\Gamma_\omega^{ee} = \Gamma_\omega \times \text{B.R.}(\omega \rightarrow e^+e^-) = (8.68 \text{ MeV})(7.38 \times 10^{-5}) = 0.641$  keV. We find the coupling strengths  $g_\rho^2/(4\pi) = \alpha^2 m_\rho/(3\Gamma_\rho^{ee}) = 1.98$  and  $g_\omega^2/(4\pi) = \alpha^2 m_\omega/(3\Gamma_\omega^{ee}) = 21.7$  using the meson parameters [23]. These coupling strengths then give the ratio of the axion-meson coupling to the axion-photon coupling [7, 23]:  $g_{A\rho\omega}/g_{A\gamma\gamma} = \sqrt{g_\rho^2/(4\pi) \times g_\omega^2/(4\pi)}/\alpha = 8.98 \times 10^2$ . The ratio allows us to evaluate the drop (See Eq. 4):  $\Delta a_\mu^{\text{HLO}} = (g_{A\rho\omega}/g_{A\gamma\gamma}) \times \Delta a_\mu \times \sqrt{NVT/(N_\mu V_\mu T_\mu)} = 0.144 \times \Delta a_\mu \times \sqrt{(N/10^{10})(V/10^{-4} \text{ cm}^3)(T/10^{-4} \text{ }\mu\text{sec})}$ , where, we have used the FNAL E989 muon beam parameters to evaluate  $N_\mu, V_\mu$ , and  $T_\mu$  [18]. Hadron production by the DAΦNE collider detected by KLOE at the  $\rho$  meson  $\pi^+\pi^-$  resonance lies close to the world average for this channel which dominates the  $a_\mu^{\text{HLO}}$  calculation within the standard model [5]. We therefore estimate the shift  $\Delta a_\mu^{\text{HLO}}$  using the electron-positron beam parameters inside KLOE at DAΦNE [24]:  $N_+ = 2.1 \times 10^{10}, N_- = 3.2 \times 10^{10}, \sigma_x = 260 \text{ }\mu\text{m}, \sigma_y = 4.8 \text{ }\mu\text{m}$ , and  $\sigma_z = 2$  cm. Combining the electron-positron beam parameters using the expressions in [21], one finds

$N = \sqrt{N_+ N_-} = 2.6 \times 10^{10}$ ,  $V = 6.3 \times 10^{-4} \text{ cm}^3$  and  $T = 1.3 \times 10^{-4} \mu\text{sec}$ . Finally, we get  $\Delta a_\mu^{\text{HLO}}(\text{KLOE}) = 0.144 \times (171 \pm 10) \times 10^{-11} \sqrt{(2.6)(6.3)(1.3)} = (114 \pm 7) \times 10^{-11}$ , where, we have used the shift  $\Delta a_\mu$  predicted using FNAL E989 beam parameters [18].

[26] R. L. Workman *et al.* (Particle Data Group), to be published in Prog. Theor. Exp Phys. **2022**, 083C01 (2022).

[27] The radio-frequency magnetic field points along the infrared electric field.

[28] M. Bialek, A. Magrez, A. Murk, and J.-Ph. Ansermet, Spin-wave resonances in bismuth orthoferrite at high temperatures, Phys. Rev. B **97**, 054410 (2018).

[29] The electromagnon  $\theta$  resonates when the terahertz electric field  $E_{\text{THz}}$  is perpendicular to the spin cycloid plane in  $\text{BiFeO}_3$ . This plane is defined by the spontaneous polarization  $P_{\text{DC}}$  and the cycloid wavevector: See Eq. (10), Fig. 2, and accompanying discussion on pg. 3 of Ref. [30]. The axion converts the magnetic field  $B_{\text{IR}}$  in the incident infrared light into a parallel terahertz frequency electric field  $E_{\text{THz}}$ . The infrared light gets absorbed when  $E_{\text{THz}}$  resonates with the electromagnon  $\theta$ . This happens when  $B_{\text{IR}}$  is perpendicular to the spin cycloid plane.

[30] R. de Sousa and J. E. Moore, Optical coupling to spin waves in the cycloidal multiferroic  $\text{BiFeO}_3$ , Phys. Rev. B **77**, 012406 (2008).